1    **Quenching of an Aniline Radical Cation by Dissolved Organic**

2    **Matter and Phenols: A Laser Flash Photolysis Study**

3

4

5    *Frank Leresche,[†,‡] Lucie Ludvíková,[⊥] Dominik Heger,*[⊥] Urs von Gunten,[†,‡] and*

6    *Silvio Canonica*[*,†]

7

8    [†]Eawag, Swiss Federal Institute of Aquatic Science and Technology, Überlandstrasse 133,

9    CH-8600 Dübendorf, Switzerland

10    [‡]School of Architecture, Civil and Environmental Engineering (ENAC), Ecole Polytechnique

11    Fédérale de Lausanne (EPFL), CH-1015 Lausanne, Switzerland

12    [⊥]Department of Chemistry, Faculty of Science, Masaryk University,

13    Kamenice 5, 62500 Brno, Czech Republic

14

15

16

17

18

19

20

21

22

23

24

25

26  **Graphical Abstract**
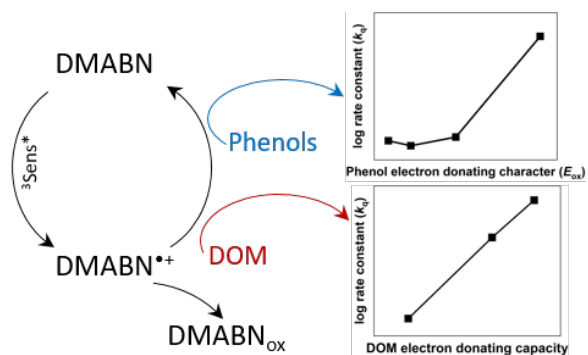


27

28      **Abstract**

29      Aromatic amines are relevant aquatic organic contaminants whose photochemical

30      transformation is affected by dissolved organic matter (DOM). The goal of this study is to

31      elucidate the underlying mechanism of the inhibitory effect of DOM on such reactions. The

32      selected model aromatic amine, 4-(dimethylamino)benzonitrile (DMABN), was submitted to

33      laser flash photolysis in the presence and absence of various model photosensitizers. The

34      produced radical cation (DMABN$^{\bullet+}$) was observed to react with several phenols and different

35      types of DOM on a time scale of ~100 µs. The determined second-order rate constants for the

36      quenching of DMABN$^{\bullet+}$ by phenols were in the range of $(1.4 - 26) \times 10^8 \ \mathrm{M}^{-1} \ \mathrm{s}^{-1}$ and increased

37      with increasing electron donor character of the aromatic ring substituent. For DOM, quenching

38      rate constants increased with the phenolic content of the DOM. These results indicate the

39      reduction of DMABN$^{\bullet+}$ to re-form its parent compound as the basic reaction governing the

40      inhibitory effect. In addition, the photosensitized oxidation of the sulfonamide antibiotic

41      sulfadiazine (SDZ) was studied. The observed radical intermediate of SDZ was quenched by

42      4-methoxyphenol less effectively than DMABN$^{\bullet+}$, which was attributed to the lower reduction

43      potential of this radical compared to DMABN$^{\bullet+}$.

## Introduction

Aromatic amines are a class of compounds often present as contaminants in the aquatic environment.[1-4] Under sunlight irradiation they can undergo both direct and indirect phototransformation,[5-10] the latter process being sensitized by dissolved organic matter (DOM).[11] Excited triplet states of DOM ($^3$DOM*) are the reactive intermediates formed upon DOM photoirradiation and are hypothesized to be mainly responsible for the DOM-photosensitized transformation of aromatic amines.[12, 13] The initiation of the transformation was attributed to a one-electron transfer from the aromatic amine to $^3$DOM*, which was assumed to generate the corresponding aminyl radical cation.[7, 14-17]

Besides acting as a photosensitizer, DOM can also inhibit the indirect phototransformation of some classes of organic contaminants, in particular aromatic amines.[7] This inhibition, initially observed for the phototransformation of target contaminants induced by the excited triplet states of model aromatic ketones, has been the subject of extensive studies in our research group during the last decade.[7, 14, 17-20] It was postulated that the inhibition, measured as a gradually decreasing transformation rate of the target contaminant with increasing DOM concentration, originates from the reduction of oxidized intermediates of the target contaminant by electron-donating (also named antioxidant) moieties of the DOM.[7, 18] The latter can be quantified using electrochemical methods as electron donating capacity (EDC),[21] a parameter that was found to be strongly correlated with the magnitude of the inhibitory effect.[20] In the case of aromatic amines, the oxidized intermediates subject to reduction are hypothesized to be the corresponding aminyl radicals or radical cations.

While numerous steady-state irradiation studies have been performed to characterize the inhibitory effect of DOM and model phenolic antioxidants on the photosensitized transformation of contaminants, the direct observation of the transient radical species formed

68 upon oxidation of the contaminant by $^3$DOM* and their reaction with DOM is still limited. The

69 quenching kinetics of the tryptophanyl radical cation, formed through photoionization of

70 tryptophan under acidic conditions (pH 3), was measured using phenolic compounds and a

71 fulvic acid as quenchers.[15] Analogous experiments were performed for several diphenylamine

72 radicals, produced by photosensitized one-electron oxidation of some fenamate-type drugs,

73 using ascorbic acid as a quencher,[22] and for the quenching of the mefenamic acid radical by

74 sesamol.[23] In a more recent study, the radical formed by one-electron oxidation of adenine by

75 the sulfate radical and subsequent deprotonation was observed to react with catechol and three

76 different purines regenerating adenine.[24] These radical kinetics data were used for an improved

77 understanding of the abatement of mixtures of contaminants in advanced oxidation processes.

78 The goal of the present study is to measure the kinetics of the reaction of a model aniline radical

79 cation with phenols and DOM. This is expected to provide an important basis to understand

80 and quantify the inhibitory effect of DOM on the photosensitized transformation of the parent

81 aniline in surface waters. The radical cation of 4-(dimethylamino)benzonitrile (DMABN),

82 DMABN$^{\bullet+}$, was selected for this investigation. DMABN$^{\bullet+}$ was produced by laser flash

83 excitation through direct photoionization or photosensitized oxidation of DMABN, as detailed

84 in a preceding study.[25] Its decay kinetics in the presence of various concentrations of some

85 phenols and a few types of DOM were measured. An additional investigation was performed

86 to characterize the kinetic behavior of the radical intermediate formed during the

87 photosensitized transformation of the sulfonamide antibiotic sulfadiazine (SDZ).

88

89 **Experimental Section**

90 **Chemicals and Solutions.** All chemicals were commercially available and used as received.

91 A complete list of chemicals is given in the Supporting Information (SI, Text S1). All

experiments were performed in phosphate-buffered water (2 mM total phosphate concentration, final pH 7.74 except when otherwise stated) using stock solutions prepared in water, except for photosensitizers. Stock solutions of the photosensitizers 1-naphthaldehyde (1-NA) and 2-acetonaphthone (2-AN) were made in acetonitrile (MeCN) because of the limited solubility of these compounds in water. The concentration of the co-solvent MeCN in sample solutions containing 1-NA or 2-NA did not exceed 1% (v/v). The water used in the experiments was obtained from an Aqua Osmotic 02A purification system. Suwannee River fulvic acid (SRFA, catalogue number 1S101F), Suwannee River humic acid (SRHA, 1S101H) and Pony Lake fulvic acid (PLFA, 1R109F) were obtained from the International Humic Substances Society (IHSS, St. Paul, Minnesota). Some relevant data regarding their chemical composition as well as optical and electrochemical properties are collected in the SI, Table S1. Stock solutions of the fulvic and humic acids were prepared at concentrations of 50–100 $mg_C$ $L^{-1}$. The carbon content of the first stock solutions of each humic substance was quantified using a total organic carbon (TOC) analyzer as described below. The concentration of subsequent stock solutions was quantified by spectrophotometry using the specific absorption coefficients (SUVA) determined for the first stock solutions at the wavelengths of 240, 260 and 280 nm (see SI, Table S1). Spectrophotometric determinations were performed after dilution of the stock solutions with unbuffered ultrapure water to reach a nominal concentration of ≈5 $mg_C$ $L^{-1}$.

A natural water sample was collected on November 14th 2014, near the outlet of Etang de la Gruère (EG) (47.2376N, 7.0494 E), a small pond (surface area ≈80'000 $m^2$) surrounded by timbers and boggy wetlands. The EG water sample was filtered on a pre-washed 0.45 μm pore size cellulose nitrate filter and stored at 4 °C in the dark. The filtrate had a DOM concentration of 22.8 $mg_C$ $L^{-1}$ (measured using the TOC analyzer) and a pH of 7.7 (see ref 17 for full characteristics of the water).

**Laser Flash Photolysis Experiments.** Nanosecond laser flash photolysis experiments using pulses of $\leq 170$ ps duration from a Nd:YAG laser were conducted as detailed elsewhere.[25] The observation wavelengths of the different transient species are given in the SI, Table S2. Absorbance values of the studied solutions were usually adjusted to $0.5 - 0.8$ (for a 1 cm optical path length) at the excitation wavelength. Solutions were either naturally aerated or purged using a gentle stream of $N_2O$ for 15 minutes prior to measurements. Absorption spectra of the photolyzed solutions were measured regularly between laser flashes to test for possible photodegradation of the solution components using the hereafter mentioned diode-array spectrophotometer. Experiments were conducted in an air-conditioned room at a temperature of $21 \pm 1$ °C.

**Kinetic Analyses.** The kinetic traces for the decay of $DMABN^{\bullet+}$ and the intermediate radical formed upon oxidation of SDZ were analyzed using the software Kintecus©[26] and the kinetic models given in the SI (Texts S2 and S3, Tables S3 and S6 for $DMABN^{\bullet+}$ and Text S7 and Table S9 for the SDZ radical). First-order decay rate constants of the excited triplet states of the studied photosensitizers were determined by fitting their decay traces to single exponential decay model functions using the software Flash Fit v. 0.11. Second-order rate constants for triplet state quenching by various phenols or SDZ were obtained as the slope of linear regression lines of the above first-order rate constants, determined for different quencher concentrations, versus the concentration of the quencher.

**Analytical Instrumentation.** Electronic absorption spectra in the ultraviolet (UV) and visible (Vis) range were measured on an Agilent Cary 100 UV-Vis or an Agilent 8654 diode-array spectrophotometer. A BNC pHTestr 10 pH meter equipped with a calibrated glass electrode or an equivalent Eutech Instruments pH600 was used to measure pH. The total organic carbon concentrations of the humic substances stock solutions and of EG water were measured as non-purgeable organic carbon, after appropriate dilution, sample acidification and online purging

142    to remove inorganic carbon, using a Shimadzu TOC-L CSH total organic carbon analyzer (limit

143    of quantification 0.5 $mg_C$ $L^{-1}$, accuracy 0.2 $mg_C$ $L^{-1}$, measuring range 0.5 – 30 $mg_C$ $L^{-1}$).

## Results and Discussion

**Radical Cation of 4-(Dimethylamino)benzonitrile (DMABN), DMABN$^{\bullet+}$.** *Kinetics of the Quenching of DMABN$^{\bullet+}$ by Phenols as Model Antioxidants.* Using the previously developed laser flash photolysis procedures,[25] DMABN$^{\bullet+}$ was generated either by direct photoionization (eq 1) or by triplet-photosensitized oxidation (eqs 2–3).

$$\text{DMABN} + h\nu \rightarrow \text{DMABN}^{\bullet+} + e_{aq}^{-} \tag{1}$$

$$\text{Sens} + h\nu \rightarrow {}^{1}\text{Sens*} \rightarrow {}^{3}\text{Sens*} \tag{2}$$

$$^{3}\text{Sens*} + \text{DMABN} \rightarrow \text{DMABN}^{\bullet+} + \text{Sens}^{\bullet-} \tag{3}$$

In these reaction equations, Sens is a photosensitizer, $^{1}$Sens* and $^{3}$Sens* are its excited singlet and triplet states, respectively, and Sens$^{\bullet-}$ is its radical anion resulting through the electron transfer from DMABN to $^{3}$Sens*. The two different methods of producing DMABN$^{\bullet+}$ were applied to check the reliability of second-order quenching rate constants obtained for some phenols. The photosensitizer method was preferred because it not only mimics the formation route of DMABN$^{\bullet+}$ in the aquatic environment, but also has the technical advantage that the excitation pulse (at a wavelength of 355 nm) is weakly absorbed by the phenolic quenchers or DOM, thus reducing the possible impact of side reactions. Moreover, the direct photoionization method (excitation wavelength of 266 nm) could not be applied when using DOM as a quencher due to excessive absorption of the laser pulse by DOM. The kinetics of the quenching of DMABN$^{\bullet+}$ by several phenols (R–PhOH) (eq 4), was studied in aqueous solutions containing an individual phenol at variable concentrations by recording kinetic traces at the observation wavelength of 500 nm, corresponding to the absorption maximum of DMABN$^{\bullet+}$.

$$\text{DMABN}^{\bullet+} + \text{R–PhOH} \rightarrow \text{DMABN} + \text{R–PhO}^{\bullet} + \text{H}^{+} \tag{4}$$

9
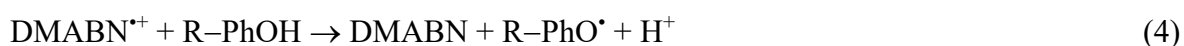
166   In eq 4, we considered the product of the one-electron oxidation of the phenol to be its phenoxyl

167   radical (R–PhO$^{\bullet}$), being aware that the corresponding phenoxyl radical cation (R–PhOH$^{\bullet+}$,

168   typical p$K_a$ values $< 0$ [27, 28]), which is not observable on the time scale of the present

169   experiments due to fast deprotonation, might be the primary reaction product. Figure 1

170   displays, as an example, a series of transient absorption traces showing the quenching of

171   DMABN$^{\bullet+}$ by 4-methoxyphenol: DMABN$^{\bullet+}$ was formed through 1-NA-photosensitized

172   oxidation of DMABN. This particular photosensitizer was selected for this study because of

173   the high second-order rate constant for the reaction of its excited triplet state, $^{3}$1-NA*, with

174   DMABN[25] and the limited reactivity of $^{3}$1-NA* with the employed phenolic quenchers (with

175   the only exception of 4-methoxyphenol, see below). The traces were measured at an

176   observation wavelength of 500 nm for various concentrations of 4-methoxyphenol in the range

177   of $0 - 3 \times 10^{-4}$ M, while the concentration of DMABN was $5.0 \times 10^{-4}$ M. A visual inspection

178   of the decay traces reveals a steady acceleration of the decay with increasing concentration of

179   4-methoxyphenol. We previously studied decays without added quencher in detail and found

180   that they approximately followed second-order kinetics, which was mainly attributed to the

181   reaction of DMABN$^{\bullet+}$ with the superoxide radical anion.[25] To take account of these kinetic

182   features, which preclude the use of exponential decay functions to correctly obtain second-

183   order quenching rate constants, the analysis of the decay traces was performed using kinetic

184   modeling (for details, see the Experimental Section and Text S2 and Table S3, SI). The signal

185   at early delay times after the laser pulse ($< 1$ μs) contains not only the contribution of

186   DMABN$^{\bullet+}$, but also the one of $^{3}$1-NA*, while the contributions of the radical anion of 1-NA,

187   i.e., 1-NA$^{\bullet-}$, and the 4-methoxyphenoxyl radical (and also of any other phenoxyl radicals

188   produced from the phenols studied here) are negligible at this wavelength. To eliminate

189   interference by $^{3}$1-NA*, only data for time delays $> 6$ μs after the laser pulse were considered

190   to extract the decay parameters of DMABN$^{\bullet+}$ (SI, Text S2). For each experimental run, second-

order quenching rate constants of DMABN$^{•+}$ by a given phenol (R−PhOH) employed at a given concentration were obtained by the described kinetic modeling procedure (see SI, Tables S4 and S5 for the whole set of data). The average values of the second-order rate constants for the quenching of DMABN$^{•+}$ by R−PhOH, termed as $k_{DMABN^{•+},R-PhOH}^{q,exp}$, are presented in Table 1 (see footnote $d$).

A series of DMABN$^{•+}$ quenching experiments using a reduced set of phenols were also performed employing direct photoionization of DMABN (eq 1). The detailed results of these experiments, evaluated by applying the kinetic modeling described in the SI (Text S3 and Table S6), are presented in the SI (Table S7), and the determined average values of $k_{DMABN^{•+},R-PhOH}^{q,exp}$ are provided in Table 1 (see footnote $e$). These values were found to agree well with those determined using the photosensitized oxidation of DMABN.
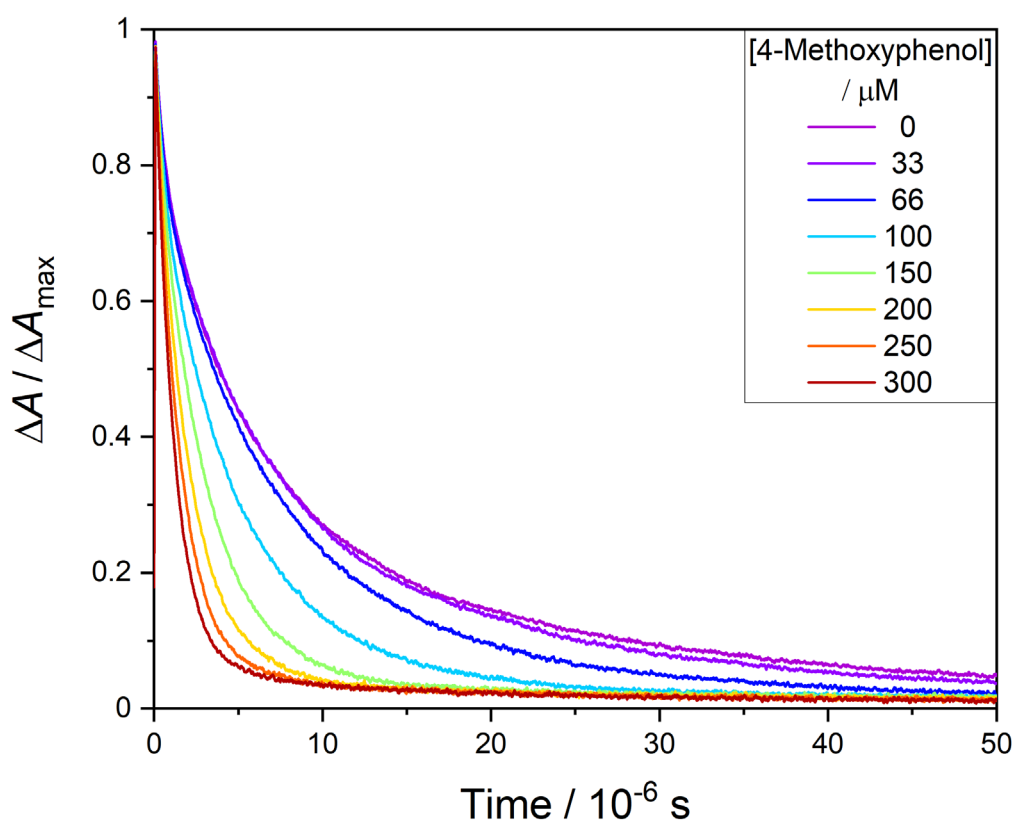
204    **Figure 1.** Quenching of DMABN$^{\bullet+}$ by 4-methoxyphenol, as shown by the kinetic traces

205    (excitation $\lambda$ = 355 nm; observation $\lambda$ = 500 nm) observed during laser flash photolysis of

206    aerated aqueous solutions containing 1-naphthaldehyde ($3.0 \times 10^{-4}$ M), DMABN ($5.0 \times 10^{-4}$

207    M) and an increasing concentration of 4-methoxyphenol in the range of

208    $0 - 3 \times 10^{-4}$ M at pH 7.74 (2 mM phosphate buffer). The transient differential absorbance data

209    ($\Delta A$) were smoothed using adjacent averaging with 50 data points (corresponding to $5 \times 10^{-8}$

210    s) and each kinetic trace was normalized to its differential absorbance maximum ($\Delta A_{\max}$).

211

**Table 1. Second-order rate constants for the quenching of DMABN$^{•+}$ and the excited triplet state of 1-naphthaldehyde (1-NA) by several phenols and types of DOM (pH 7.74).**

| Phenol substituent (R) | $E^0_{ox}$ [a] / V vs. SHE | $k^{q,exp}_{DMABN^{•+},R-PhOH}$ [b] / $10^8$ M$^{-1}$ s$^{-1}$ | $k^{q,exp}_{^31-NA^*,R-PhOH}$ [c] / $10^8$ M$^{-1}$ s$^{-1}$ |
|---|---|---|---|
| 4-OCH$_3$ | -1.23 | 17 ± 2,[d] 26 ± 8 [e] | 39 ± 7 |
| 4-OCH$_3$ (D$_2$O) | n.a. [f] | 23 ± 1 [d] | 8 ± 3 |
| 3-OH | n.a. | 3.2 ± 1.3,[d] 4.1 ± 0.4 [e] | 1.2 ± 0.3 |
| 4-CH$_3$ | -1.38 | 1.7 ± 0.4 [d] | 0.7 ± 0.5 |
| 4-(CH$_3$)$_3$C | -1.46 | 1.4 ± 0.4 [d] | 0.7 ± 0.4 |
| none | -1.50 | 1.6 ± 0.6,[d] 2.1± 0.2 [e] | 0.5 ± 0.2 |
| none (D$_2$O) | n.a. | 0.5 ± 0.2 [d] | < 0.5 [g] |

| DOM | EDC [h] / μmol$_{e-}$ mg$_C^{-1}$ | $k^{q,exp}_{DMABN^{•+},DOM}$ [b] / $10^3$ L mg$_C^{-1}$ s$^{-1}$ | $k^{q,exp}_{DMABN^{•+},EDM}$ [i] / $10^8$ M$^{-1}$ s$^{-1}$ | $k^{q,exp}_{^31-NA^*,DOM}$ [c] / $10^7$ L mol$_C^{-1}$ s$^{-1}$ |
|---|---|---|---|---|
| SRHA | 7.01 | 8.2 ± 1.1 [d] | 11.7 ± 1.6 | 4.8 ± 2.4 |
| SRFA | 5.43 [j] | 4.9 ± 0.9 [d] | 8.9 ± 1.7 | 3.6 ± 2.4 |
| PLFA | 2.29 | 1.6 ± 0.4 [d] | 7.0 ± 1.7 | 11 ± 8 |
| Etang de la Gruère | n.a. | 4.1 ± 1.5 [d] | n.a. | 8.4 ± 7.2 |

215 $^a$ Set equal to the negative value of the standard one-electron reduction potential for the couple

216 R–PhOH$^{\bullet+}$/R–PhOH from Ref. [29]; unit: V vs. standard hydrogen electrode (SHE). $^b$ Second-

217 order rate constant for the quenching of DMABN$^{\bullet+}$ by R–PhOH or DOM (mean ± standard

218 deviation) obtained by averaging the constants from individual decay traces according to SI,

219 Tables S4, S5, or S7. $^c$ Second-order rate constant for the quenching of the excited triplet state

220 of 1-naphthaldehyde by R–PhOH or DOM (mean ± 95% confidence interval) obtained from

221 decay traces measured at $\lambda_{obs} = 600$ nm and the methods described in the Experimental Section.

222 $^d$ Values obtained by 1-naphthaldehyde photosensitized formation of DMABN$^{\bullet+}$

223 (355 nm laser excitation, aerated solution). $^e$ Values obtained by direct photoionization of

224 DMABN (266 nm laser excitation, N$_2$O-purged solution). $^f$ n.a.: not available. $^g$ Value too low

225 for quantification. $^h$ Electron donating capacity (EDC) calculated using data from ref [21] and

226 carbon content from ref [30]. $^i$ Ratio between $k_{\text{DMABN}^{\bullet+},\text{DOM}}^{\text{q,exp}}$ and EDC. $^j$ EDC value for the SRFA

227 (II) isolate was used.

228

229 The obtained $k_{\text{DMABN}^{\bullet+},\text{R–PhOH}}^{\text{q,exp}}$ values (see Table 1) vary by about an order of magnitude among

230 the studied phenols. At the higher end, 4-methoxyphenol exhibits a second-order rate constant

231 of $\approx 2 \times 10^9$ M$^{-1}$ s$^{-1}$, which may be considered as nearly diffusion controlled. At the lower end,

232 phenol and the two alkyl-substituted phenols have very similar second-order rate constants, on

233 average $\approx 1.6 \times 10^8$ M$^{-1}$ s$^{-1}$, while resorcinol shows an intermediate value. Since the reaction

234 of DMABN$^{\bullet+}$ with phenols is postulated to involve an electron transfer from the phenols to

235 DMABN$^{\bullet+}$ (eq 4), a positive correlation between $k_{\text{DMABN}^{\bullet+},\text{R–PhOH}}^{\text{q,exp}}$ and the standard one-

236 electron oxidation potential ($E_{ox}^0$) of the phenols is expected. When inspecting the values of

237 $E_{ox}^0$ for the non-dissociated phenols given in Table 1, it can be deduced that there is no

238 significant influence of $E_{ox}^0$ on the second-order rate constants of phenol and the alkyl-

239 substituted phenols. However, a large increase in the second-order rate constants occurs when

240 $E_{ox}^0$ increases from -1.38 to -1.23 V vs. standard hydrogen electrode (SHE) (the $E_{ox}^0$ values for

241 4-methylphenol and 4-methoxyphenol, respectively). The negative value of the standard one-

242 electron reduction potential of DMABN (1.30 ± 0.07 V vs. SHE, taken as the average of two

243 values recently estimated from excited triplet quenching data using a Rehm-Weller

244 relationship),[25] falls near the middle of the range in which the jump in second-order rate

245 constant occurs. Consequently, a pure electron transfer reaction of the type:

246 $DMABN^{•+} + R–PhOH \rightarrow DMABN + R–PhOH^{•+}$ (5)
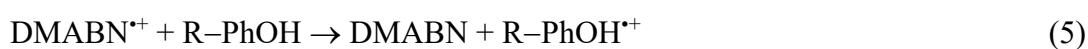
247 would be exergonic for 4-methoxyphenol, thus explaining the nearly diffusion-controlled rate

248 constant, but endergonic for the three other phenols at the lower end of the reactivity scale, also

249 in line with the determined second-order rate constants for these phenols.

250 For 4-methoxyphenol and phenol the effect of deuteration of the phenolic group was evaluated

251 using heavy water ($D_2O$) as a solvent to obtain possible indications about the mechanism of

252 their reaction with $DMABN^{•+}$. The deuterium isotope effect, i.e., $k_{DMABN^{•+},R–PhOH}^{q,exp}/$

253 $k_{DMABN^{•+},R–PhOD}^{q,exp}$, obtained from the values given in Table 1 is near unity (0.7) for

254 4-methoxyphenol and ≈3.2 for phenol. These different values are in line with a pure one-

255 electron transfer mechanism in the first case, and the involvement of a proton transfer in the

256 rate determining step of the reaction in the second case, supporting a proton-coupled electron

257 transfer mechanism.[31]

258 One important side-reaction that may affect the formation of $DMABN^{•+}$ by $^3Sens^*$, in particular

259 by $^31-NA^*$, is the quenching of these excited triplet states by phenols (or DOM, *vide infra*).

260 This process can on the one hand reduce the formation rate of $DMABN^{•+}$ and on the other hand

261 lead to the formation of reaction intermediates (specifically, phenoxyl radicals), possibly

262 complicating the determination of the rate constants for DMABN$^{\bullet+}$. Phenoxyl radicals are

263 known to be formed in high yields during quenching of $^3$Sens*,[29, 32] according to eq 6.

264 $$^3\text{Sens*} + \text{R–PhOH} \rightarrow \,^3\text{Sens}^- + \text{R–PhO}^\bullet + \text{H}^+ \qquad (6)$$
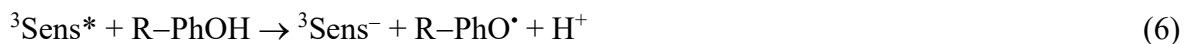
265 For several phenols, $^3$Sens* second-order quenching rate constants have been measured for

266 three aromatic ketones[29] and methylene blue[16] as photosensitizers. For the set of phenols used

267 in the present study, we determined the second-order $^3$1-NA* quenching rate constants (see

268 Table 1) employing the phenols in the same concentration ranges as detailed in Table S4 (SI).

269 These second-order rate constants fit the trends of triplet state reductive quenching by

270 phenols.[29] However, they are higher than the ones determined for the excited triplet state of

271 2-acetonaphthone,[29] which indicates that the latter should have a slightly lower reduction

272 potential than $^3$1-NA*, although the values that can be deduced from literature are the same

273 (i.e., 1.34 V vs. SHE).[25] While 4-methoxyphenol exhibits a high second-order rate constant

274 near the diffusion-controlled limit and close to the one previously determined for DMABN

275 $(3.4 \times 10^9 \text{ M}^{-1} \text{ s}^{-1})$,[25] the other phenols possess second-order quenching rate constants

276 $\leq 1.2 \times 10^8 \text{ M}^{-1} \text{ s}^{-1}$. Despite these relatively low values, at the higher concentrations of the

277 phenols used in the DMABN$^{\bullet+}$ quenching experiments (i.e., up to $4 \times 10^{-3}$ M), the phenols may

278 compete significantly with DMABN for reaction with $^3$1-NA*. For this reason, not only the

279 reaction of DMABN with $^3$1-NA*, but also the reaction of the phenols with $^3$1-NA* (see eqs 3

280 and 6, respectively) was included in the kinetic model to obtain quenching rate constants of

281 DMABN$^{\bullet+}$ (see SI, Table S3).

282 *Product Formation during the Reaction of DMABN$^{\bullet+}$ with Phenol.* The expected primary

283 products of this reaction (eq 4) on the applied experimental time scale are the parent compound

284 (DMABN) and the phenoxyl radical derived from the selected phenol. Figure 2 illustrates the

285 formation of the phenoxyl radical by laser flash photolysis ($\lambda = 355$ nm) of solutions containing

286    2-acetonaphthone (2-AN) or 1-NA as photosensitizers and phenol in the absence or presence

287    of DMABN. Excitation of 2-AN or 1-NA in the presence of phenol yields their excited triplet

288    states, with absorption maxima at $\approx$440 nm (Figure 2A) and $\approx$510 nm (Figure 2C),

289    respectively.[25] The evolution of the triplet state spectra in the presence of phenol is almost

290    identical compared to a solution containing the photosensitizers alone,[25] reflecting the very low

291    triplet quenching rate constants by phenol ($3.3 \times 10^7$ M$^{-1}$ s$^{-1}$ for $^3$2-AN*[29] and $5 \times 10^7$ M$^{-1}$ s$^{-1}$

292    for $^3$1-NA*, see Table 1). The only found difference consist in the appearance of weak

293    absorption features in the wavelength range of 390 $-$ 460 nm at longer delay times after the

294    laser pulse. In Figure 2C, two peaks can be clearly distinguished in this wavelength range. The

295    first peak, at $\approx$400 nm, can be assigned to the absorption of the phenoxyl radical, PhO$^\bullet$.[33, 34]

296    The origin of the second peak, at $\approx$430 nm, is uncertain. In view of the sub-micromolar

297    concentration of PhO$^\bullet$, coupling of two phenoxyl radicals can be excluded on the time scale of

298    $10^{-5}$ s, which leaves an adduct of the type PhOH$-$PhO$^\bullet$ as a possible candidate. Such radical

299    adducts have been proposed to occur in very acidic solution.[34] In addition, an absorption band

300    in the same spectral region was also observed (but not discussed) in a study involving the

301    formation of PhO$^\bullet$.[35] Furthermore, the absorption of the 4-phenoxyphenoxyl radical also

302    matches the $\approx$430 nm peak,[36] supporting our suggested adduct formation.

303    In the transient absorption spectra of a solution containing one of the photosensitizers, together

304    with phenol and DMABN (Figure 2B, D), the excited triplet state absorption band decreases

305    more rapidly than in the absence of DMABN. Moreover, the characteristic absorption of

306    DMABN$^{\bullet+}$ with a maximum at $\approx$500 nm becomes clearly visible at $\approx$1 $\mu$s delay time. At

307    intermediate time delays a transient absorption with maximum at $\approx$420 nm is visible (Figure

308    2D). This is caused by the radical anion of 1-NA, which is formed concomitantly with

309    DMABN$^{\bullet+}$ (see eq 3) and disappears within < 10 $\mu$s due to scavenging by oxygen (to form 1-

NA and superoxide). The corresponding radical anion of 2-AN in Figure 2B is less visible owing to the strong superposition of its absorption band with the one of $^3$2-AN*.[25] At the longest time delays (12 – 15 $\mu$s) the DMABN$^{\bullet+}$ signal has almost disappeared and only the absorption features attributed to the phenoxyl radical remain. These bands have a much higher intensity than those detected in the absence of DMABN (Figures 2A, C), demonstrating the oxidation of phenol by DMABN$^{\bullet+}$ to yield PhO$^{\bullet}$ as described by eq 4. Interestingly, an additional weak shoulder at $\approx$450 nm and 15 $\mu$s time delay is visible in Figure 2D, which might also be due to phenoxyl radical adducts of the type discussed above.
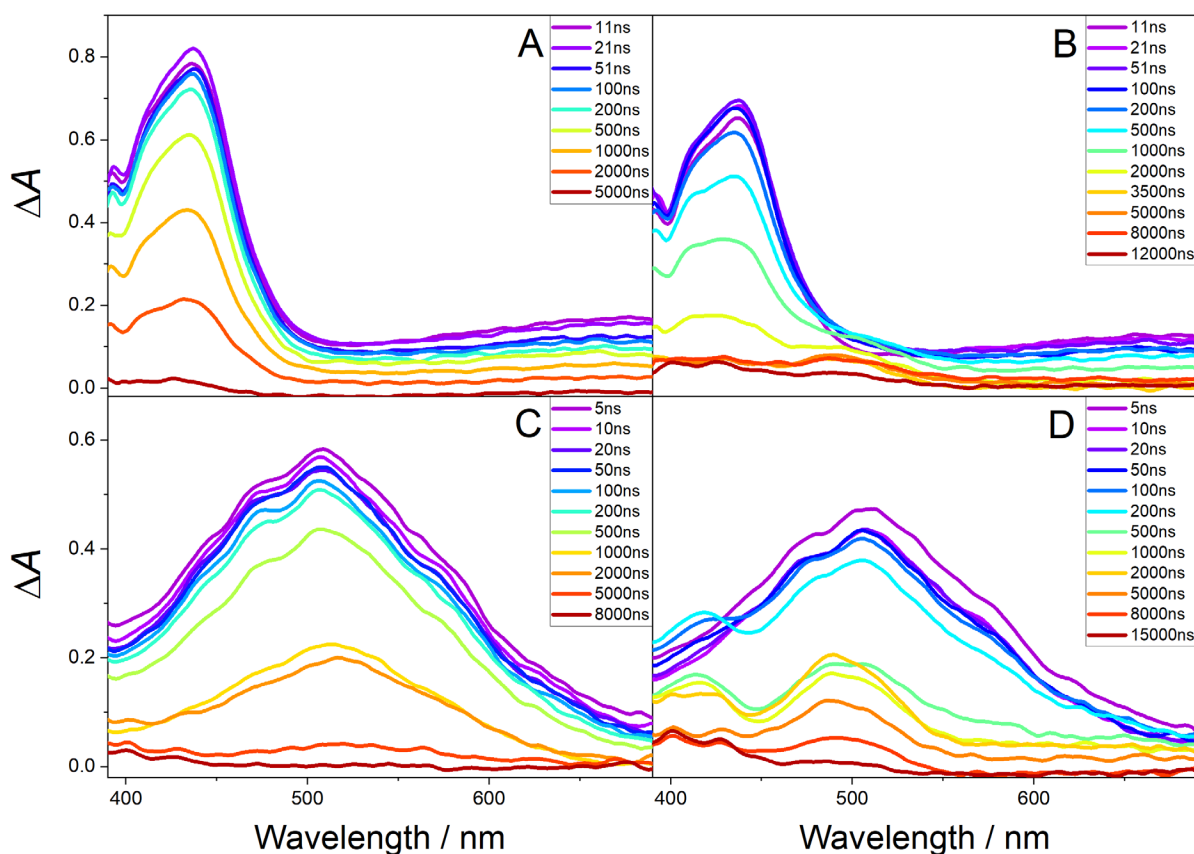


**Figure 2.** Transient absorption spectra following 355 nm laser pulse excitation of aqueous solutions containing: (A) 2-Acetonaphthone (2-AN) and phenol; (B) 2-AN, DMABN, and phenol; (C) 1-Naphthaldehyde (1-NA) and phenol; (D) 1-NA, DMABN, and phenol. Concentration of the components: $5.0 \times 10^{-4}$ M for 2-AN, phenol, and DMABN; $3.0 \times 10^{-4}$ M

324  for 1-NA. All solutions contained $\approx$1% (v/v) MeCN and were buffered at pH 7.74 (2 mM

325  phosphate). Spectral data were smoothed by adjacent averaging over 20 data points ($\approx$10 nm).

326  *Kinetics of the Quenching of DMABN$^{\bullet+}$ by DOM.* Similar to experiments with phenols, the

327  decay of DMABN$^{\bullet+}$ formed through 1-NA photosensitization was accelerated by the presence

328  of DOM (Figure 3). Second-order rate constants for the quenching of DMABN$^{\bullet+}$ by DOM

329  ($k_{\mathrm{DMABN}^{\bullet+},\mathrm{DOM}}^{\mathrm{q,exp}}$, Table 1) were obtained using kinetic modeling (see SI, Text S2 and Table S3),

330  analogously as for quenching by phenols. Considering the chemical complexity of DOM

331  solutions, the quality of fits was satisfactory despite some deviations for low DOM

332  concentrations (see SI, Figure S2). It is noteworthy that quenching of $^3$1-NA* by DOM in the

333  concentration range used in this study is negligible, wherefore no adverse effect of this reaction

334  on the determination of $k_{\mathrm{DMABN}^{\bullet+},\mathrm{DOM}}^{\mathrm{q,exp}}$ is expected. This can be deduced from the determined

335  second-order triplet quenching rate constants ($k_{^3\text{1-NA}^*,\mathrm{DOM}}^{\mathrm{q,obs}}$, Table 1), which are low and in

336  agreement with the triplet quenching results obtained for other photosensitizers.[37] Values of

337  $k_{\mathrm{DMABN}^{\bullet+},\mathrm{DOM}}^{\mathrm{q,exp}}$ were found to lie in the range of $(1.6 - 8.2) \times 10^3 \, \mathrm{mg_C^{-1} \, L \, s^{-1}}$. To our knowledge,

338  the only published second-order rate constant for an analogous reaction was determined for the

339  quenching of the tryptophan radical cation by SRFA at pH 3[15] and determined as $(1.1 \pm 0.2) \times$

340  $10^4 \, \mathrm{mg_C^{-1} \, L \, s^{-1}}$, i.e., $\approx$2.2 times higher than $k_{\mathrm{DMABN}^{\bullet+},\mathrm{SRFA}}^{\mathrm{q,exp}}$.

341  For solutions of the DOM isolates, $k_{\mathrm{DMABN}^{\bullet+},\mathrm{DOM}}^{\mathrm{q,exp}}$ values increased with increasing electron

342  donating capacity (EDC) of these materials. The observed trend concurs with one of the main

343  hypotheses regarding the inhibitory effect of DOM on excited triplet induced oxidations. This

344  hypothesis postulates the reduction of oxidation intermediates, in the present case DMABN$^{\bullet+}$,

345  by antioxidant moieties of the DOM. For the natural water from Etang de la Gruère (for which

346  no EDC value is available) the second-order quenching rate constant falls between the

corresponding values for SRFA and PLFA (Table 1). Electron-donating moieties (EDMs) in the DOM are expected to play a central role in determining the reactivity of DOM towards DMABN$^{•+}$. Therefore, it is useful to define a second-order rate constant expressing the reactivity in terms of EDMs. This rate constant, $k_{DMABN^{•+},EDM}^{q,exp}$, was approximated by dividing $k_{DMABN^{•+},DOM}^{q,exp}$ by the EDC of each specific DOM, being aware that EDC values may be higher than predicted by a 1:1 stoichiometry with electron donating phenolic moieties.[38] The corresponding values (in units of $M^{-1}s^{-1}$, see the third column in Table 1) are significantly different among the three DOM extracts and increase in the order PLFA < SRFA < SRHA, which may indicate that the strength of the EDMs (i.e., their ability to donate electrons) in each DOM increases in the same order. Moreover, the reactivity of EDMs towards DMABN$^{•+}$ is comprised in the range spanned by the model phenols (upper part of Table 1), being closer to the one of 4-methoxylphenol than the one of phenol and the alkyl-substituted phenols. These relatively high values of $k_{DMABN^{•+},EDM}^{q,exp}$ might be partly related to the higher fraction, at pH 7.74, of the deprotonated form in the phenolic moieties of the DOM as a consequence of their lower average $pK_a$[39] compared to the phenols investigated here. In view of the relatively high reactivity of EDMs compared to model phenols, a possible reduced access of DMABN$^{•+}$ to EDMs, caused by steric hindrance or limited diffusivity of DMABN$^{•+}$ in the vicinity of complex DOM molecules or aggregates, does not appear to be relevant.
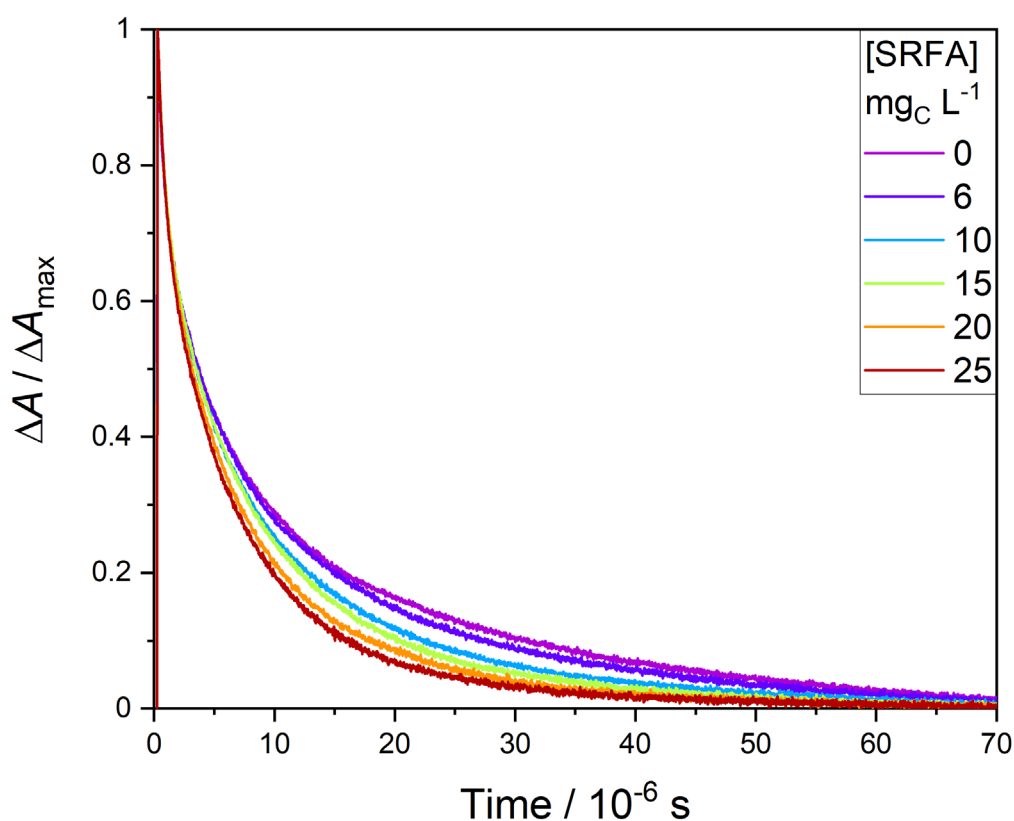
366

**Figure 3.** Quenching of DMABN$^{\bullet+}$ by Suwannee River fulvic acid (SRFA), as shown by the kinetic traces (excitation $\lambda = 355$ nm; observation $\lambda = 500$ nm) observed during laser flash photolysis of aerated aqueous solutions containing 1-naphthaldehyde ($3.0 \times 10^{-4}$ M), DMABN ($5.0 \times 10^{-4}$ M) and an increasing concentration of SRFA in the range of $0 - 25$ mg$_C$ L$^{-1}$. The transient differential absorbance data ($\Delta A$) were smoothed using adjacent averaging with 50 data points (corresponding to $5 \times 10^{-8}$ s) and each kinetic trace was normalized to its differential absorbance maximum ($\Delta A_{max}$).

*Relationship between DMABN$^{\bullet+}$ Second-Order Quenching Rate Constants and the Inhibitory Effect of Phenols and DOM on the Phototransformation of DMABN.* The observed reactivity of DMABN$^{\bullet+}$ with various phenols and DOM is *per se* an important piece of evidence that the reduction of DMABN$^{\bullet+}$ by these electron-donating compounds may be associated with their

379      inhibitory effect on the photosensitized transformation of DMABN.[17] We briefly recall the

380      simplest kinetic model used to explain this inhibitory effect, consisting in the formation of a

381      reaction intermediate (probably DMABN$^{•+}$ in this case), which can either react to yield

382      transformation products of DMABN or undergo reduction by electron-donating compounds (a

383      phenol or antioxidant moieties of DOM), thus reforming DMABN. The competition between

384      reduction and transformation of DMABN$^{•+}$ leads to a decreased phototransformation rate of

385      DMABN compared to the case in the absence of antioxidants. The relevant kinetic constants

386      obtained in the present and a previous study[25] are the first-order rate constant for the decay of

387      DMABN$^{•+}$ in the absence of quenchers, $k_{DMABN^{•+}}^{d,0}$ , and the second-order rate constants for the

388      quenching of DMABN$^{•+}$ by phenols or DOM, $k_{DMABN^{•+},R-PhOH}^{q,exp}$ or $k_{DMABN^{•+},DOM}^{q,exp}$ . Assuming

389      that DMABN$^{•+}$ is the key intermediate for the inhibitory effect, the following relationships can

390      be derived:

391      $$[R-PhOH]_{1/2} = k_{DMABN^{•+}}^{d,0} / k_{DMABN^{•+},R-PhOH}^{q,exp} \qquad (7)$$

392      $$[DOM]_{1/2} = k_{DMABN^{•+}}^{d,0} / k_{DMABN^{•+},DOM}^{q,exp} \qquad (8)$$

393      where $[R-PhOH]_{1/2}$ and $[DOM]_{1/2}$ are the concentrations of a given phenol or DOM,

394      respectively, needed to reduce the first-order phototransformation rate constant of DMABN by

395      50% compared to the case in the absence of R–PhOH or DOM (the derivation of these

396      equations is provided in refs 7, 14, 18). Using the rate constants given in Table 1 and the

397      previously determined estimates of $k_{DMABN^{•+}}^{d,0}$, i.e. $(4.8 \pm 1.2) \times 10^3$ s$^{-1}$ and $(3.5 \pm 1.4) \times 10^3$ s$^{-1}$

398      from direct photoionization and photosensitized oxidation of DMABN, respectively,[25] the

399      following values can be obtained by applying eqs 7 or 8: $[PhOH]_{1/2} = (23 \pm 6)$ μM, $(22 \pm 12)$

400      μM; $[PLFA]_{1/2} = (3.0 \pm 1.1)$ mg$_C$ L$^{-1}$, $(2.2 \pm 1.0)$ mg$_C$ L$^{-1}$; $[SRFA]_{1/2} = (0.98 \pm 0.30)$ mg$_C$ L$^{-1}$,

401      $(0.7 \pm 0.3)$ mg$_C$ L$^{-1}$. For the fulvic acids there is a reasonable agreement with the values

402 obtained from steady-state irradiations ([PLFA]$_{1/2}$ = (3.2 ± 1.2) mg$_C$ L$^{-1}$; [SRFA]$_{1/2}$ = (1.5 ±

403 0.4) mg$_C$ L$^{-1}$),[17] but [PhOH]$_{1/2}$ for the steady-state irradiation value, i.e. (3.7 ± 1.2) μM, is by

404 a factor of ≈6 lower than estimated using eq 7. The reason for this discrepancy is not understood

405 at the moment.

406

407 **Sulfadiazine.** Several studies have shown that the triplet-induced oxidation of this sulfonamide

408 antibiotic is inhibited by DOM and model phenolic antioxidants.[7, 14, 19] To elucidate the

409 mechanism of the inhibitory effect for SDZ, analogous experiments as for DMABN were

410 carried out.

411 In a first step, for the excited triplet state of several photosensitizers the quenching induced by

412 SDZ was investigated with the aim of determining the corresponding second-order rate

413 constants, $k^{\text{q,exp}}_{^3\text{Sens*,SDZ}}$, and subsequently estimate the one-electron standard oxidation potential

414 of SDZ (see the SI, Text S4). In this study, we focus on the anionic species of sulfadiazine,

415 SDZ$^-$, which is the prevalent species at pH 7.74 (p$K_a$ = 6.4).[6] The measurement of $k^{\text{q,exp}}_{^3\text{Sens*,SDZ}}$

416 for a set of photosensitizers with triplet-state reduction potential ($E^{0*}_{\text{red}}$) in the range of 1.26 −

417 1.71 V vs. SHE yielded values in the range of 2.9 × 10$^7$ M$^{-1}$ s$^{-1}$ to 2.8 × 10$^9$ M$^{-1}$ s$^{-1}$ (see SI,

418 Table S8). $k^{\text{q,exp}}_{^3\text{Sens*,SDZ}}$ increased nonlinearly with $E^{0*}_{\text{red}}$. Moreover, $k^{\text{q,exp}}_{^3\text{Sens*,SDZ}}$ values were

419 consistently lower than the corresponding $k^{\text{q,exp}}_{^3\text{Sens*,DMABN}}$ values. Assuming a reductive

420 quenching of the excited triplet states by SDZ$^-$ in analogy to DMABN (see eq 3), the second-

421 order rate constant data were fitted using the Rehm-Weller relationship for one-electron

422 transfer reactions (SI, eq S1 and Figure S6),[25] yielding $E^0_{\text{red}}$(SDZ$^\bullet$/SDZ$^-$) = 1.28 ± 0.20 V vs.

423 SHE, where SDZ$^\bullet$ represents the primary radical resulting from one-electron oxidation of

424    SDZ$^-$. Despite the large uncertainty, this value is very close to the value of $1.30 \pm 0.07$ V vs.

425    SHE for $E^0_{red}(\text{DMABN}^{\bullet+}/\text{DMABN})$ determined in a preceding study.[25]

426    In a second step, we characterized the species involved in the reductive quenching of the

427    excited triplet state of 1-NA by SDZ (see SI, Text S5 and Figure S7). The reaction of SDZ with

428    the excited triplet state of two photosensitizers produced a broad transient absorption spectrum

429    centered at $\approx$430 nm attributed to SDZ$^{\bullet-}$, the radical resulting from deprotonation of SDZ$^{\bullet}$

430    according to a previous quantum chemical computation study.[40] This transient species decayed

431    with a first-order rate constant of $(1.7 - 2) \times 10^3$ s$^{-1}$.

432    Finally, the observation of the reaction of SDZ$^{\bullet-}$ with various phenols and DOM isolates was

433    attempted, but successful only for the case of 4-methoxyphenol, for which second-order rate

434    constants of $(1.0 \pm 0.2) \times 10^8$ M$^{-1}$ s$^{-1}$ for an aqueous solution and $(8 \pm 3) \times 10^7$ M$^{-1}$ s$^{-1}$ for a D$_2$O

435    solution were determined (see SI, Texts S6 and S7, Tables S9 and S10, and Figure S8). The

436    lack of deuterium isotope effect suggests a one-electron transfer mechanism without

437    involvement of the phenolic proton for this reaction. The significantly lower reactivity of SDZ$^{\bullet-}$

438    compared to DMABN$^{\bullet+}$ supports the assignment of this species, which is the product of the

439    deprotonation of SDZ$^{\bullet}$ and has consequently a lower one-electron reduction potential than

440    SDZ$^{\bullet}$ and DMABN$^{\bullet+}$. The failure to detect a quenching of SDZ$^{\bullet-}$ by the other selected phenols

441    or DOM is probably due to the low absorption signal of the SDZ$^{\bullet-}$. Furthermore, in the case of

442    the phenols, the second-order rate constants are expected to be lower than the quantification

443    limit of $\approx$10$^7$ M$^{-1}$ s$^{-1}$ for the used experimental conditions.

444    Despite the low reactivity of SDZ$^{\bullet-}$ with phenols (and probably DOM) compared to DMABN$^{\bullet+}$,

445    the triplet-induced transformation of SDZ under steady-state irradiation has been shown in

446    several studies to be subject to a relevant inhibition by phenols or DOM,[14, 19, 41] with

447    $[R - PhOH]_{1/2}$ values of similar magnitude as for DMABN.[17] Considering eqs 7 and 8, one

448    can conclude that similar $[R - PhOH]_{1/2}$ values for SDZ and DMABN can only be obtained if

449    the relaxation constant of SDZ$^{\bullet-}$, $k_{SDZ^{\bullet-}}^{d,0}$, is much slower than for DMABN$^{\bullet+}$. Since the first-

450    order relaxation rate constants for DMABN$^{\bullet+}$ and SDZ$^{\bullet-}$ determined by LFP are in the same

451    order of magnitude, we hypothesize that LFP probably overestimates the value of $k_{SDZ^{\bullet-}}^{d,0}$ .


452


453    **Environmental Implications**


454    In the present study, we were able to measure the reaction kinetics of DMABN$^{\bullet+}$, an example

455    of aromatic aminyl radical cations, with various model phenols and different types of DOM.

456    The positive correlation of the observed DMABN$^{\bullet+}$ second-order quenching rate constants with

457    the oxidation potentials of the model phenols and the electron donating capacity of DOM

458    strongly suggests that DMABN$^{\bullet+}$ is reduced to its parent compound, DMABN. These

459    observations reinforce the hypothesis put forward in a previous paper[7] that the inhibitory effect

460    of DOM on the photosensitized transformation of certain aquatic contaminants, in particular

461    aromatic amines, may be due to the reduction of oxidized intermediates of these contaminants

462    by antioxidant moieties in the DOM. Notably, the relevance of the inhibitory effect of DOM is

463    not restricted to aquatic photochemistry, but may extend to a variety of reactions induced by

464    oxidizing radicals, as recently demonstrated for the oxidative transformation of various anilines

465    and sulfonamide antibiotics by the sulfate radical.[42]


466    A more stringent test of the validity of the model describing the inhibitory effect consists in

467    utilizing the rate constants obtained from the kinetic studies of the radical cation (in the present

468    case DMABN$^{\bullet+}$) to calculate the extent of the inhibitory effect and comparing predicted and

469    experimental values.[17] As discussed above, the prediction was successful for DOM, but

470    overestimated by a factor of $\approx$6 [PhOH]$_{1/2}$, the central parameter describing the inhibitory effect

471   of phenol. This discrepancy is not massive in view of the errors affecting the determination of

472   the various kinetic constants by laser flash photolysis and steady-state irradiation, but could

473   indicate that side-reactions of DMABN$^{\bullet+}$ not considered in the simple kinetic model may

474   influence the inhibitory effect. In a recent study of the inhibitory effect of DOM on oxidations

475   induced by the sulfate radical,[42] 5 – 7 times lower $[DOM]_{1/2}$ values were determined for the

476   transformation of the sulfonamide antibiotic sulfamethoxazole compared to the values obtained

477   for triplet-induced oxidation.[18] This difference was attributed to possible side-reactions caused

478   by the superoxide radical anion in triplet-induced oxidations. These observations call for a

479   detailed examination of the role of superoxide, and possibly further transient reducing species

480   formed under irradiation of DOM, in aquatic photochemistry.[43]

481   The modest results obtained in the present study for sulfadiazine preclude a prediction of the

482   inhibitory effect on its photosensitized transformation, because the rate constants of the

483   corresponding intermediate radical are missing. The example of sulfadiazine demonstrates that

484   laser flash photolysis is not always a suitable tool to understand and predict the inhibitory effect

485   of phenols and DOM on the indirect phototransformation of relevant aquatic contaminants.

486   Future developments in the field of quantum chemical computations[44] might provide

487   alternative methods to reach this objective.

488

489   **Associated content**

490   Supporting Information.

491   The Supporting Information is available free of charge on the ACS Publications website at

492   DOI:.........

493       Details on chemicals, organic matter isolates, and a natural water sample; laser flash

494       photolysis parameters; additional text sections, tables and figures regarding the

495        determination of quenching rate constants for the radicals of DMABN and SDZ and

496        for the excited triplet states of photosensitizers

497

498   **Author information**

499   *Corresponding Authors:

500   SC: Telephone: +41-58-765-5453. Fax +41-58-765-5028. E-mail: silvio.canonica@eawag.ch.

501   DH: Telephone: +420 54949 3322. E-mail: hegerd@chemi.muni.cz.

502   Notes: The authors declare no competing financial interests.

503

508

509   **References**

510   1.    Stone, W. W.; Gilliom, R. J.; Ryberg, K. R. Pesticides in U.S. streams and rivers:

511   Occurrence and trends during 1992-2011. *Environ. Sci. Technol.* **2014,** *48* (19), 11025-11030.

512   2.    Schäfer, R. B.; von der Ohe, P. C.; Kühne, R.; Schüürmann, G.; Liess, M. Occurrence

513   and toxicity of 331 organic pollutants in large rivers of North Germany over a decade (1994 to

514   2004). *Environ. Sci. Technol.* **2011,** *45* (14), 6167-6174.

515   3.    Moschet, C.; Wittmer, I.; Simovic, J.; Junghans, M.; Piazzoli, A.; Singer, H.; Stamm,

516   C.; Leu, C.; Hollender, J. How a complete pesticide screening changes the assessment of

517   surface water quality. *Environ. Sci. Technol.* **2014,** *48* (10), 5423-5432.

518   4.    Miao, X. S.; Bishay, F.; Chen, M.; Metcalfe, C. D. Occurrence of antimicrobials in the

519   final effluents of wastewater treatment plants in Canada. *Environ. Sci. Technol.* **2004,** *38* (13),

520   3533-3541.

521     5.      Werner, J. J.; McNeill, K.; Arnold, W. A. Environmental photodegradation of

522     mefenamic acid. *Chemosphere* **2005,** *58* (10), 1339-1346.

523     6.      Boreen, A. L.; Arnold, W. A.; McNeill, K. Triplet-sensitized photodegradation of sulfa

524     drugs containing six-membered heterocyclic groups: Identification of an $SO_2$ extrusion

525     photoproduct. *Environ. Sci. Technol.* **2005,** *39* (10), 3630-3638.

526     7.      Canonica, S.; Laubscher, H.-U. Inhibitory effect of dissolved organic matter on triplet-

527     induced oxidation of aquatic contaminants. *Photochem. Photobiol. Sci.* **2008,** *7* (5), 547-551.

528     8.      Guerard, J. J.; Miller, P. L.; Trouts, T. D.; Chin, Y. P. The role of fulvic acid

529     composition in the photosensitized degradation of aquatic contaminants. *Aquat. Sci.* **2009,** *71*

530     (2), 160-169.

531     9.      Ratti, M.; Canonica, S.; McNeill, K.; Bolotin, J.; Hofstetter, T. B. Isotope fractionation

532     associated with the indirect photolysis of substituted anilines in aqueous solution. *Environ. Sci.*

533     *Technol.* **2015,** *49* (21), 12766-12773.

534     10.     Othmen, K.; Boule, P. Photochemical behaviour of dichloroanilines in water and

535     formation of aminochlorophenoxazones. *J. Photochem. Photobiol. A-Chem.* **1999,** *121* (3),

536     161-167.

537     11.     Richard, C.; Canonica, S. Aquatic phototransformation of organic contaminants

538     induced by coloured dissolved natural organic matter. In *The Handbook of Environmental*

539     *Chemistry*, Hutzinger, O., Ed. Springer: Berlin, Germany, 2005; Vol. 2, Part M, pp 299-323.

540     12.     Canonica, S. Oxidation of aquatic organic contaminants induced by excited triplet

541     states. *Chimia* **2007,** *61* (10), 641-644.

542     13.     McNeill, K.; Canonica, S. Triplet state dissolved organic matter in aquatic

543     photochemistry: reaction mechanisms, substrate scope, and photophysical properties. *Environ.*

544     *Sci.: Processes Impacts* **2016,** *18* (11), 1381-1399.

545     14.     Wenk, J.; Canonica, S. Phenolic antioxidants inhibit the triplet-induced transformation

546     of anilines and sulfonamide antibiotics in aqueous solution. *Environ. Sci. Technol.* **2012,** *46*

547     (10), 5455-5462.

548     15.     Janssen, E. M. L.; Erickson, P. R.; McNeill, K. Dual roles of dissolved organic matter

549     as sensitizer and quencher in the photooxidation of tryptophan. *Environ. Sci. Technol.* **2014,**

550     *48* (9), 4916-4924.

551 16. Erickson, P. R.; Walpen, N.; Guerard, J. J.; Eustis, S. N.; Arey, J. S.; McNeill, K.
552 Controlling factors in the rates of oxidation of anilines and phenols by triplet methylene blue
553 in aqueous solution. *J. Phys. Chem. A* **2015,** *119* (13), 3233-3243.

554 17. Leresche, F.; von Gunten, U.; Canonica, S. Probing the photosensitizing and inhibitory
555 effects of dissolved organic matter by using *N,N*-dimethyl-4-cyanoaniline (DMABN). *Environ.*
556 *Sci. Technol.* **2016,** *50* (20), 10997-11007.

557 18. Wenk, J.; von Gunten, U.; Canonica, S. Effect of dissolved organic matter on the
558 transformation of contaminants induced by excited triplet states and the hydroxyl radical.
559 *Environ. Sci. Technol.* **2011,** *45* (4), 1334-1340.

560 19. Bahnmüller, S.; von Gunten, U.; Canonica, S. Sunlight-induced transformation of
561 sulfadiazine and sulfamethoxazole in surface waters and wastewater effluents. *Water Res.*
562 **2014,** *57*, 183-192.

563 20. Wenk, J.; Aeschbacher, M.; Sander, M.; von Gunten, U.; Canonica, S. Photosensitizing
564 and inhibitory effects of ozonated dissolved organic matter on triplet-induced contaminant
565 transformation. *Environ. Sci. Technol.* **2015,** *49* (14), 8541-8549.

566 21. Aeschbacher, M.; Graf, C.; Schwarzenbach, R. P.; Sander, M. Antioxidant properties
567 of humic substances. *Environ. Sci. Technol.* **2012,** *46* (9), 4916-4925.

568 22. Davis, C. A.; Erickson, P. R.; McNeill, K.; Janssen, E. M. L. Environmental
569 photochemistry of fenamate NSAIDs and their radical intermediates. *Environ. Sci.: Processes*
570 *Impacts* **2017,** *19* (5), 656-665.

571 23. Davis, C. A.; McNeill, K.; Janssen, E. M. L. Non-singlet oxygen kinetic solvent isotope
572 effects in aquatic photochemistry. *Environ. Sci. Technol.* **2018,** *52* (17), 9908-9916.

573 24. Cheng, S. S.; Lei, Y.; Lei, X.; Pan, Y. H.; Lee, Y.; Yang, X. Coexposure degradation
574 of purine derivatives in the sulfate radical-mediated oxidation process. *Environ. Sci. Technol.*
575 **2020,** *54* (2), 1186-1195.

576 25. Leresche, F.; Ludvíková, L.; Heger, D.; Klán, P.; von Gunten, U.; Canonica, S. Laser
577 flash photolysis study of the photoinduced oxidation of 4-(dimethylamino)benzonitrile
578 (DMABN). *Photochem. Photobiol. Sci.* **2019,** *18* (2), 534-545.

579 26. Ianni, J. C. *Kintecus*, Windows, version 5.20; 2014.

580    27.    Dixon, W. T.; Murphy, D. Determination of the acidity constants of some phenol radical
581    cations by means of electron spin resonance. *J. Chem. Soc. Faraday Trans. 2* **1976,** *72*, 1221-
582    1230.

583    28.    Holton, D. M.; Murphy, D. Determination of acid dissociation constants of some phenol
584    radical cations. Part 2. *J. Chem. Soc. Faraday Trans. 2* **1979,** *75*, 1637-1642.

585    29.    Canonica, S.; Hellrung, B.; Wirz, J. Oxidation of phenols by triplet aromatic ketones in
586    aqueous solution. *J. Phys. Chem. A* **2000,** *104* (6), 1226-1232.

587    30.    http://humic-substances.org/elemental-compositions-and-stable-isotopic-ratios-of-
588    ihss-samples/ (01/15/2020),

589    31.    Sjödin, M.; Ghanem, R.; Polivka, T.; Pan, J.; Styring, S.; Sun, L. C.; Sundström, V.;
590    Hammarström, L. Tuning proton coupled electron transfer from tyrosine: A competition
591    between concerted and step-wise mechanisms. *Phys. Chem. Chem. Phys.* **2004,** *6* (20), 4851-
592    4858.

593    32.    Das, P. K.; Bhattacharyya, S. N. Laser flash photolysis study of electron transfer
594    reactions of phenolate ions with aromatic carbonyl triplets. *J. Phys. Chem.* **1981,** *85* (10), 1391-
595    1395.

596    33.    Ye, M. Y.; Madden, K. P.; Fessenden, R. W.; Schuler, R. H. Azide as a scavenger of
597    hydrogen atoms. *J. Phys. Chem.* **1986,** *90* (21), 5397-5399.

598    34.    Das, T. N. Oxidation of phenol in aqueous acid: Characterization and reactions of
599    radical cations vis-à-vis the phenoxyl radical. *J. Phys. Chem. A* **2005,** *109* (15), 3344-3351.

600    35.    Mvula, E.; Schuchmann, M. N.; von Sonntag, C. Reactions of phenol-OH-adduct
601    radicals. Phenoxyl radical formation by water elimination *vs.* oxidation by dioxygen. *J. Chem.*
602    *Soc.-Perkin Trans. 2* **2001,** (3), 264-268.

603    36.    De Laurentiis, E.; Socorro, J.; Vione, D.; Quivet, E.; Brigante, M.; Mailhot, G.;
604    Wortham, H.; Gligorovski, S. Phototransformation of 4-phenoxyphenol sensitised by 4-
605    carboxybenzophenone: Evidence of new photochemical pathways in the bulk aqueous phase
606    and on the surface of aerosol deliquescent particles. *Atmos. Environ.* **2013,** *81*, 569-578.

607    37.    Wenk, J.; Eustis, S. N.; McNeill, K.; Canonica, S. Quenching of excited triplet states
608    by dissolved natural organic matter. *Environ. Sci. Technol.* **2013,** *47* (22), 12802-12810.

609 38. Walpen, N.; Schroth, M. H.; Sander, M. Quantification of phenolic antioxidant moieties
610 in dissolved organic matter by flow-injection analysis with electrochemical detection. *Environ.*
611 *Sci. Technol.* **2016,** *50* (12), 6423-6432.

612 39. Ritchie, J. D.; Perdue, E. M. Proton-binding study of standard and reference fulvic
613 acids, humic acids, and natural organic matter. *Geochim. Cosmochim. Acta* **2003,** *67* (1), 85-
614 96.

615 40. Tentscher, P. R.; Eustis, S. N.; McNeill, K.; Arey, J. S. Aqueous oxidation of
616 sulfonamide antibiotics: Aromatic nucleophilic substitution of an aniline radical cation. *Chem.-*
617 *Eur. J.* **2013,** *19* (34), 11216-11223.

618 41. Vione, D.; Fabbri, D.; Minella, M.; Canonica, S. Effects of the antioxidant moieties of
619 dissolved organic matter on triplet-sensitized phototransformation processes: Implications for
620 the photochemical modeling of sulfadiazine. *Water Res.* **2018,** *128*, 38-48.

621 42. Canonica, S.; Schönenberger, U. Inhibitory effect of dissolved organic matter on the
622 transformation of selected anilines and sulfonamide antibiotics induced by the sulfate radical.
623 *Environ. Sci. Technol.* **2019,** *53* (20), 11783-11791.

624 43. Chen, Y.; Zhang, X.; Feng, S. X. Contribution of the excited triplet state of humic acid
625 and superoxide radical anion to generation and elimination of phenoxyl radical. *Environ. Sci.*
626 *Technol.* **2018,** *52* (15), 8283-8291.

627 44. Tentscher, P. R.; Lee, M.; von Gunten, U. Micropollutant oxidation studied by quantum
628 chemical computations: Methodology and applications to thermodynamics, kinetics, and
629 reaction mechanisms. *Accounts Chem. Res.* **2019,** *52* (3), 605-614.

630